Synthesis and Characterization of Large Particle Size Self-Matting Core-shell Acrylic Resin

by

Hao Peng,[1] Huan Wei,[1] Jun Xiang,[1] Yi Chen,[1] and Haojun Fan[1,2]*

[1]*Key Laboratory of Leather Chemistry and Engineering of Ministry of Education, Sichuan University,* Chengdu 610065, China

[2]*State Key Laboratory of Polymer Materials Engineering, Sichuan University*, Chengdu 610065, China

Abstract

Acrylic resin plays an important role in leather-making, such as finishing agent, filler and tanning agent. Acrylic resin can be easily fabricated via conventional emulsion polymerization, but how to prepare large particle size with self-matting effect has always been a challenge. In this paper, a continuous three-stage polymerization method: seed-polymerization coupled core-polymerization and shell polymerization was employed to prepare large particle size self-matting acrylic resin emulsion. Simultaneously, the effect of feeding methods on particles size and the effects of latex particle size, shell structure and cross-linking degree on the morphology and gloss of coating were investigated. The Z-average size of PBA seed latex particles was 213.4 nm for semi-continuous feeding method but 82.3nm for batch feeding method. After three-time continuous growth, the seed emulsion turned into core emulsion, and the particle size of core latex reached about 700nm. In third stages of shell polymerization, the core emulsion was changed into core-shell emulsion, and the latex particle size increased further to 804nm. The latex particle size, core-shell structure and cross-linking degree of shell layer were found to influence the gloss of the coating. Large latex particle size imparted the film spherical micro-rough surface, soft-core combined with hard-shell structure led to deformation resistant during film formation and cross-linking of shell layer increased the densification of shell layer, all contributed to the coating rough surface, as a result, increasing the matting effect of the coating. Finally, the leather gloss was reduced from 5.8° to 1.2°.

Introduction

The preparation method of acrylic resins was invented by the German scientist Rohm in the early 20th century and used as a leather finishing agent in Germany in the 1930s.[1] Acrylic resin has good oxidation resistance and medium resistance because the C-C single bond in its main chain is difficult to be oxidized and hydrolyzed. At the same time, the main absorption peak of C-C single bond to electromagnetic wave is not in the range of solar spectrum, so it has good outdoor weather resistance. In addition, acrylic resin emulsion has the advantage of simple production process, safety, environment friendly, and low cost.[2-4] Therefore, it has been widely used in leather finishing, textile laminating, interior and exterior wall coating, adhesive, papermaking, automobile, construction, aerospace and other fields.[4-5]

As a coating material, acrylic resin plays a special role in protection, decoration and other aspects such as hydrophobicity and antifouling.[6] The gloss of the coating can be divided into matting coating and bright coating determined by their reflectivity to light. Bright coating has a crystal clear and beautiful appearance, so it is a popular choice for young consumers. With the changed aesthetic concept, people begin to pay more attention to the introverted fashion beauty. In recent years, the matting coating with soft luster has been widely used in automotive interior leather, sofa leather, wood painting, etc, which greatly promotes the development of matting coating materials.[7]

According to the Bennet-Porteus rough surface light reflection model,[8] the relationship between light reflectivity R of the rough surface with the mean square roughness R_q of the coating surface is shown as in formula 1,

$$R = R_0\, exp\left[-\left(\frac{4\pi R_q cosi}{\lambda}\right)^2\right] \quad (1)$$

Where R_0 represents the reflectivity of absolutely flat surface, i is incident angle and λ is the wavelength of incident light.

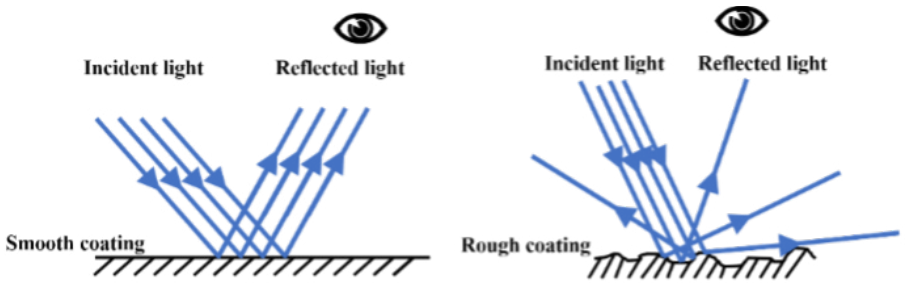

Figure 1. Effect of coating surface roughness on light path

*Corresponding author email: fanhaojun@scu.edu.cn

Manuscript received January 23, 2022, accepted for publication March 22, 2022.

The propagation path of light on surface is shown in Figure 1. When a beam of incident light is emitted to the coating surface, light interacts with the coating, some will be absorbed, and some will be reflected and refracted. For the extremely smooth surface, the angle of incident light is the same as that of reflected light, which leads to a complete reflection and a high-gloss coating. In turn, for the rough surface, due to different normal directions of each point on the surface, many light beams diffuse on the surface, so the light intensity entering eyes becomes weaker and the matting effect is obtained.[9,10]

The conventional matting coating is obtained by adding matting fillers into polymer bulk. These matting fillers are usually inorganic silica powder or organic wax powder, and their particle sizes are larger than the latex particles, which will produce uneven surface after film-forming.[11,12] However, the poor compatibility between them will inevitably bring a series of problems, such as poor stability of emulsion, poor appearance of coating, rough handle and low transmittance.[7,11,12] Therefore, self-matting acrylic resin and polyurethane have become a research hotspot.[10,13,14] Such polymers are usually prepared into larger particle size emulsions, forming rough surfaces when film forming, resulting in matting effect. As well known that the preparation of acrylic resin emulsion is classical emulsion polymerization, the latex particle size synthesized by this method is too small (50-150nm) to meet the requirement for extinction. Therefore, how to prepare large size latex through special emulsion polymerization is the key issue to the preparation of self-matting acrylic resin.

According to the film-forming mechanism of polymer emulsion as illustrated in Figure 2, the film formation process of acrylic resin emulsion can be divided into three steps. (1)Firstly, moisture volatilization in the polymer emulsion, the latex particles gradually accumulate, water and other soluble substances are dispersed in the gap between the latex particles. (2) With the further volatilization of water, the gap between latex particles becomes smaller until a capillary is formed. The capillary action forces the latex particles to deform, resulting in disappearance of the interface between particles. (3) Finally, the polymer chains diffuse and entangle at the interface of raw latex particles, and the particles fuse with each other to form a continuous and flat polymer film.[15-17] In the film-forming process, the soft latex particles are prone to deformation in the second stage of film formation and fusion in the third step, resulting in a relatively smooth and high gloss surface. However, as a matting coating, the deformation and fusion of latex particles should be avoided as much as possible in the process of film formation, so as to improve the roughness of the coating and obtain the matting effect. Therefore, hard latex particles are more suitable for matting coating.

For this reason, a large particle size self-matting acrylic resin emulsion with soft core and hard shell was prepared by three-stage-method. Firstly, butyl acrylate (BA) was used as soft monomer to prepare PBA seed emulsion with particle size of about 200nm. Then, the core latex was prepared by three-time core polymerization on the basis of seed emulsion to enlarge the particle size of latex to approximately 700nm. Finally, P (BA-MMA/AN) soft core-hard shell latex with latex particle size of 800nm was obtained by shell polymerization with methyl methacrylate (MMA) and propylene cyanide (AN) as hard monomers. At the same time, the effects of feeding method of monomer and emulsifier and the growing method of seed latex particle on latex particle size and the effects of latex particle size, shell hardness and crosslinking on the gloss of the coating were also investigated.

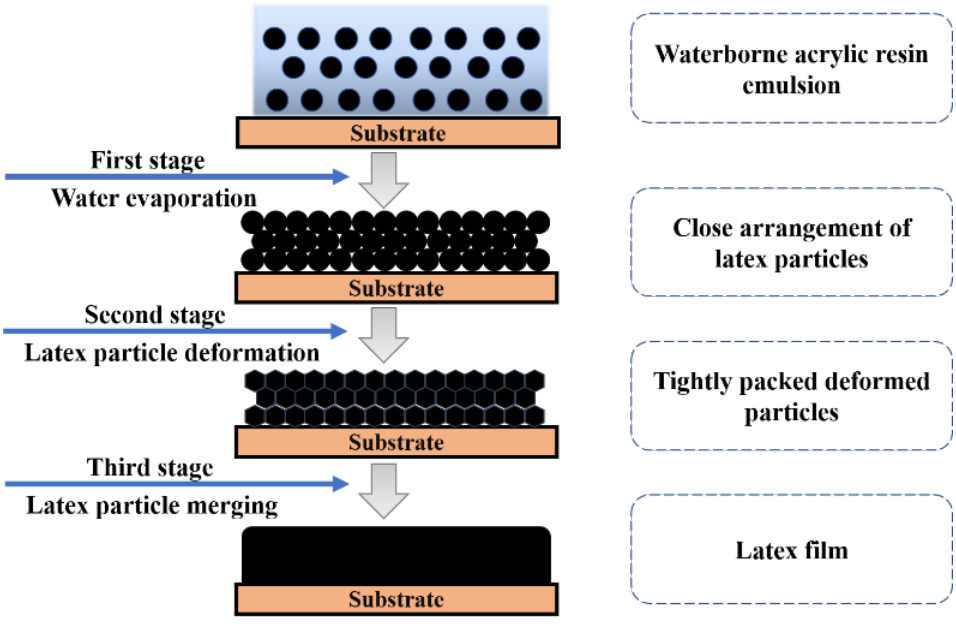

Figure 2. Film formation process of acrylic resin emulsion

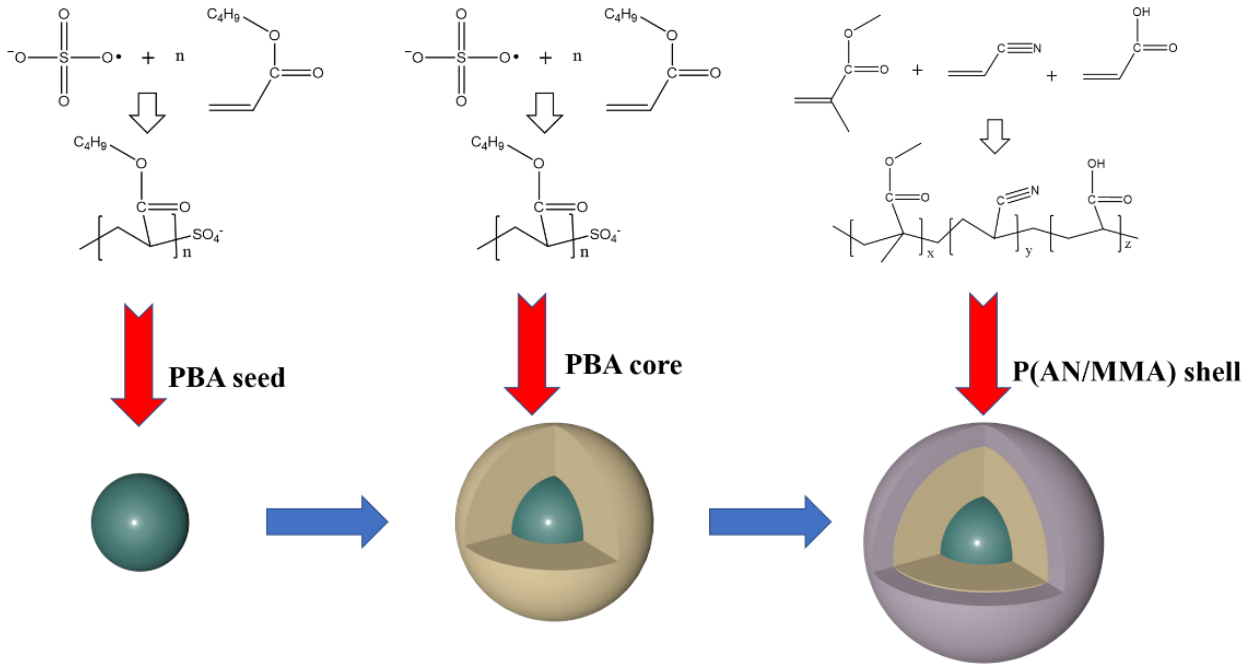

Figure 3. Synthesis of acrylic resin emulsion latex particle

Experiment

Raw materials

Butyl acrylate (BA) was purchased from Greagent. Methyl methacrylate (MMA), acrylic acid (AC), allyl methacrylate (AMA) and sodium dodecyl sulfate (SDS) were purchased from Adamas. Acrylonitrile (AN) was purchased from TCI. Deionized water (DDI) was self-made in the laboratory as the synthesis medium.

Preparation of acrylic resin emulsion

The preparation of acrylic resin emulsion was divided into three stages. Firstly, the PBA seed emulsion with relatively large particle size was prepared. Then the seed emulsion grew for three times to fabricate large particle size core emulsion. Finally, core-shell emulsion was fabricated by shell polymerization on the basis of core emulsion. In experiment, BA was used as soft monomer and MMA/AN was used as hard monomer, the amount of emulsifier SDS was low to prevent the formation of new micelles and latex particles. The specific reaction process was shown in Figure 3.

Preparation of PBA seed emulsion

The reaction was carried out in four-necked round bottom flask equipped with condensing pipes, nitrogen protection devices and mechanical stirrer. In the reaction, four-necked round bottom flask was placed in a water bath with thermostatic control. The polymerization temperature was 78°C and the stirring rate was 125rpm. According to the formula of reactants listed in Table I, the seed emulsion was first prepared. The seed emulsion was synthesized by two feeding methods under the conditions mentioned above: batch feeding method and semi-continuous feeding method. Batch feeding method, that is, all reactants were one-time poured to the reactor at the beginning polymerization. After heating to the reaction temperature, the initiator APS was added. While for semi-continuous feeding method, the pre-emulsion (BA monomer, half of the total amount of deionized water, emulsifier SDS and initiator APS) was pre-emulsified at ambient temperature for 1h firstly, then the pre-emulsion was dropped into reactor for 2h, and the seed emulsion was obtained.

Preparation of PBA core growth emulsion

Core emulsion was fabricated by three times growth of seed emulsion. According to the reactant formula listed in Table II, firstly, all BA, deionized water, SDS and APS were magnetically stirred at ambient temperature for 1h to prepare the pre-emulsion. Then the seed emulsion was poured into reactor simultaneously and heated to the reaction temperature to 75°C. After that, the pre-emulsion was dropped to the reaction system in a period of 2 h. Finally, a core emulsion with once growth of latex particles

Table I

Recipes for the preparation of PBA seed latexes

Ingredients	BA(g)	H_2O(g)	SDS(g)	APS(g)	$NaHCO_3$(g)
Seed	80	240	0.24	0.24	0.5

Table II

Recipes for the preparation of PBA core latexes

Ingredients	Seed (g)	Core1 (g)	Core2 (g)	BA (g)	H_2O (g)	SDS (g)	APS (g)	$NaHCO_3$ (g)
Core1	120	-	-	80	240	0.24	0.24	0.5
Core2	-	120	-	80	240	0.24	0.24	0.5
Core3	-	-	120	80	240	0.24	0.24	0.5

was obtained (named core 1). Similarly, core 1 was used as mother liquor, core 2 emulsion with twice growth of latex particles was prepared. In the same way, core 3 emulsion with large particles size could be achieved

Preparation of P(BA-MMA/AN) core-shell emulsion

The formulation of P(BA-MMA/AN) core-shell emulsion was shown in Table III. Firstly, the shell monomer (MMA and AN), AMA (crosslinker), deionized water, SDS and APS were magnetically stirred at ambient temperature for 1h to prepare the pre-emulsion. Then the quantitative core 3 emulsion was charged into reactor simultaneously and heated to the reaction temperature to 75°C. Finally, the pre-emulsion was dropped to the reaction system for 2 h and the P(BA-MMA/AN) emulsion with soft core and hard shell was obtained.

Preparation of leather coating

Appropriate amount of core-shell acrylic resin emulsion, leveling agent and thicker were mixed together with viscosity of 1000-1500mPa·S. Then the thickened acrylic resin was applied on leather by using 8μm rod coater. Finally, the coated leather was dried in an oven at 120°C for 5 minutes to obtain the coated leathers.

Characterization

Coating gloss test

According to the standard ISO 2813-2014, the gloss of leather coated with different acrylic resins was measured by 60° gloss meter (REFO 60, German). All samples were measured 5 times and the average value was recorded.

Measurement of latex particle size distribution

The latex particle size distribution (PSD) of acrylic resin emulsion was observed by dynamic light scattering particle size analyzer (DLS Malvern Zetasizer Nano ZS, England). The sample was diluted 500 times by deionized water in glass cuvette to determine the Z-average particle size and particle size distribution.

Characterization of surface morphology and roughness

The surface morphology and roughness of self-matting acrylic resin coating were characterized by scanning electron microscope (SEM Helios G4 UC, German) and atomic force microscope (AFM SPM-9500, Japan) respectively. The emulsion was dripped onto the silicon wafer and dried at ambient temperature and ventilation condition to obtain the coating. After spraying gold, the surface morphology of the coating was obtained by secondary electron signal of SEM. In addition, the three-dimensional surface topography and surface roughness of coating can be observed by AFM with 5μm × 5μm scanning area. The samples were prepared by spin coating self-matting acrylic resin emulsion on the silicon wafer substrate.

Characterization of glass transition temperature

The glass transition temperature (T_g) of PBA core latex and core-shell latex were characterized by differential scanning calorimetry (DSC 214 F1, NETZSCH Instrument, German). The experiment was

Table II

Recipes for the preparation of P(BA-MMA/AN) core-shell latexes

Ingredients	Core3 (g)	MMA (g)	AN (g)	AA (g)	AMA (g)	H_2O (g)	SDS (g)	APS (g)	$NaHCO_3$ (g)
Core-shell without AMA	60	15	20	0.105	0	105	0.105	0.105	0.2
Core-shell with AMA	60	15	20	0.105	0.25	105	0.105	0.105	0.2

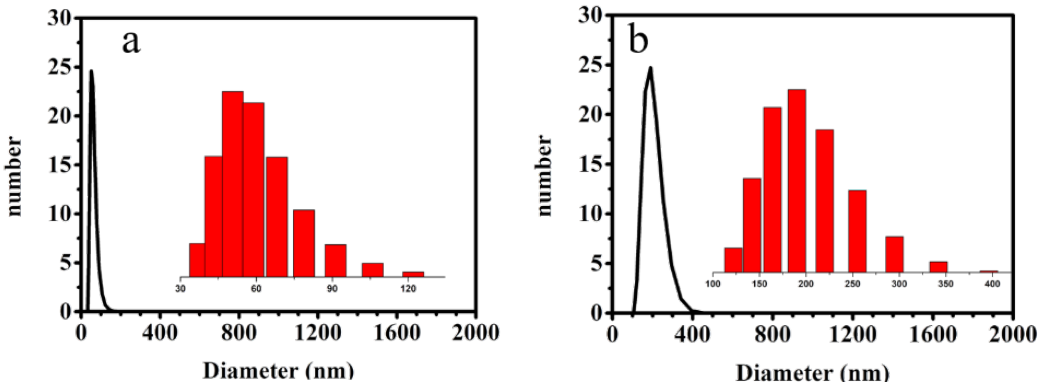

Figure 4. Particle size distribution of PBA seed latex particles: **(a)** batch **(b)**semi-continuous

carried out in nitrogen atmosphere. After eliminating the thermal history, the sample was scanned from -80°C to 160°C at a heating rate of 10°C/min.

Result and Discussion

Effect of feeding mode on particle size of seed emulsion

The particle size of the seed emulsions synthesized by two different feeding methods are shown in Figure 4. The Z-average particle size of PBA seed emulsion synthesized by batch feeding method was 82.3nm, as shown in Figure 4(a). Meanwhile, this value for semi-continuous feeding method was 213.4nm, as shown in Figure 4(b), which indicates that semi continuous feeding method is more conducive to the formation of large size seed emulsion.

The conventional free radical emulsion polymerization includes three stages according to the monomer conversion rate. Stage I: latex particle formation stage, stage II: latex particle growing stage, stage III: polymerization completion stage.[20,21] In stage I, the nucleation mechanism of latex particles can be divided into the following three types: a) micelle nucleation mechanism, b) monomer droplet nucleation mechanism and c) oligomer nucleation mechanism.

In this study, the concentration of emulsifier (SDS) in the reaction system and pre-emulsion was lower than its critical micelle concentration ($CMC_{(SDS)}$=8mmol/L). Therefore, micelles would not be formed and micelle nucleation would not occur in the reaction system.[18] For conventional radical emulsion polymerization, when the monomer droplet concentration was too low, the free radical would be hard to diffuse into monomer droplets, so monomer droplet nucleation is also difficult to occur.[19] In the aqueous phase, there were a small amount of free monomers existing as true solution, these monomers can be initiated by free radicals. Because the solubility of this polymer in aqueous phase decreased sharply with the increase of relative molecular mass, the free radical chains were precipitated before they grow to a relatively large relative molecular mass. The precipitated oligomers absorbed emulsifier from the surrounding so that it could stably exist in the aqueous phase, thus forming new latex particles. This nucleation mode is called oligomer nucleation mechanism. The formation of PBA latex particles in this experiment should follow this nucleation mechanism.

As described above, when the concentration of emulsifier (SDS) was lower than $CMC_{(SDS)}$, there were almost no micelles in the reaction system, that means the polymerization reaction went directly to stage 2 without going through stage 1, in which latex particle nucleation and latex particle growth occurred simultaneously. a) BA monomer dissolved in aqueous was initiated by free radicals in the aqueous phase to form oligomers, once their relative molecular mass became large, they would precipitate from the aqueous phase and adsorbed emulsifiers to form latex particles, i.e., oligomer nucleation. b) the radical chain formed after the reaction between APS and BA is hydrophobic at one end and hydrophilic at the other end, so the radical chain exhibited surface active, and the hydrophobic end of this surface-active radical chains entered the latex particles and triggered the monomers swelling inside the latex particles, leading to the growth of the latex particles. In above both reactions, reaction a) led to the formation of new latex particles while reaction b) led to the growth of latex particles. Therefore, if the polymeric parameters could be adjusted to make reaction b) more likely to occur, then a larger particle size emulsion could be obtained.

The possibility of oligomer nucleation can be predicted according to the number density of BA monomers in the aqueous phase. For batch feeding method, the concentration of the low water-soluble monomer BA remained constant at the beginning of the reaction, i.e., the saturation concentration of BA ($1.4\times10^{3}g{\cdot}mL^{-1}$). These monomer molecules in the aqueous phase could be triggered by free radicals for polymerization, and then the monomers in the monomer droplets would continuously diffuse into the aqueous phase to replenish the monomers consumed by polymerization, thus keeping the monomer concentration in the aqueous phase constant at the saturation concentration of BA. In the case of batch feeding method, the molecular number density N_m(batch) of BA in the aqueous [22] phase can be calculated from Equation 2:

$$N_m(\text{batch}) = \frac{1.4\times10^{-3}}{M_{BA}} \times N_A = 6.576\times10^{18} mL^{-1} \quad (2)$$

Where M_{BA} is the BA molecular mass (128.17 g/mol) and N_A represents Avogadro constant.

For semi-continuous feeding method, the number density of monomers in the aqueous phase of reaction system depended on the addition rate of monomer in the pre-emulsion. After the dropwise addition of a small amount of BA monomer, the concentration of BA monomer in the reaction system was lower than the saturation concentration of BA monomer in the aqueous phase, which means that any slowly added monomer would diffuse and be consumed rapidly in the reaction system without causing monomer enrichment. In the case of semi-continuous feeding method, the molecular number density N_m(semi-continuous) of BA[22] in the aqueous phase can be calculated from Equation 3:

$$N_m(\text{semi-continuous}) = \frac{FR_{BA}}{V_{H_2O}M_{BA}} \times N_A \leq 2.617 \times 10^{17} mL^{-1} \cdot s^{-1} \quad (3)$$

Where the FR_{BA} is the feeding rate of BA monomer in pre-emulsion, and the is the volume of deionized water initially added in the semi-continuous method.

The results obtained from the above two equations show that the molecular number density of monomer BA in semi-continuous feeding method was significantly lower than that in batch feeding method. Moreover, as the volume of the aqueous phase in the reaction system increased, the number density of BA molecules decreased further, which reduced the probability of oligomer nucleation in the semi-continuous feeding method. Therefore, the number of latex particles produced in semi-continuous feeding method was smaller and the latex particle size was larger compared to batch feeding method.

Based on the latex particle size D measured by DLS (Figure 4), the individual latex particle mass m and the latex particle number density N could be calculated by Equation 4 and Equation 5 as follows [22]

$$m = \rho\left[\frac{4}{3}\pi(D/2)^3\right] = \frac{\rho\pi D^3}{6} \quad (4)$$

$$N = \frac{M}{mV} \quad (5)$$

Where ρ is polymer density ($\rho_{PBA} = 1.08 g \cdot mL^{-1}$) and M is the total mass of monomer fed to the reactor in this stage. When the monomer conversion is 100%, the N obtained from the calculations was shown in Table IV.

The data of latex particles number density in Table IV show that in the seed emulsion preparation stage, the number density of latex particles using batch feeding method was greater than that of semi-continuous feeding method, which also confirmed the theoretical prediction in the foregoing.

Growth of Core latex particle size

In the latex particle growing stage from seed emulsion to core emulsion, the continuous feeding method was used to increase the latex particle size. After three times growth, the particle size and size distribution of the core emulsion obtained for each time is shown in Figure 5.

It can be seen that the latex particle size gradually increased with the increase of growing times, and the resultant Z-average particle size reaches about 700nm after three times of growth, which is three times that of seed latex particles. And with the increase of latex

Table IV

Diameter and number density of PBA seed latex particles at termination stage of polymerization

Seed latex particle		
Feeding Method	**Diameter(nm)**	**Number density(nm)**
Batch	82.3	1.06×10^{15}
Semi-continuous	213.4	6.07×10^{13}

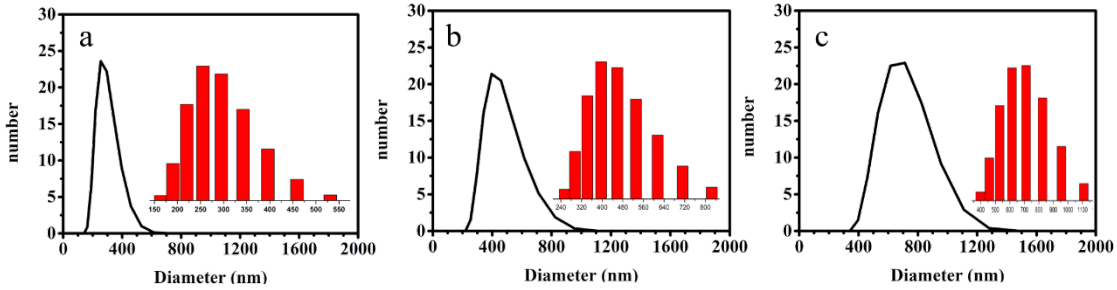

Figure 5. Particle size distribution of PBA core latex particles: **(a)** core1 **(b)** core2 **(c)** core3

Table V

Variation of diameter and number density of PBA after growth

Core latex particle		
Code	**Diameter(nm)**	**Number density**
Core-1	312.3	1.94×10^{13}
Core-2	480.4	5.32×10^{12}
Core-3	695.0	1.76×10^{12}

Table VI

The number of PBA particles at initiation and termination stage of polymerization

Code	The number of latex particles	
	Initiation of polymerization	**Termination of polymerization**
Core-1	5.46×10^{15}	6.4×10^{15}
Core-2	1.75×10^{15}	1.76×10^{15}
Core-3	4.79×10^{14}	5.81×10^{14}

particle size, the latex particle size distribution (PSD) became wider. The diameter and number density of latex particles for each growth shown in Table V.

It can be seen that the number density of latex particles decreased with each latex particle growth, which also led to the increase of latex particle size. The reason for this phenomenon was that when the continuous feeding method was adopted, some of the newly added monomers entered the interior of the latex particles and some monomers were dissolved in the aqueous phase, forming a dynamic balance of monomer concentration. According to the rule of "the likes dissolve each other", hydrophobic BA was more likely to enter the latex particles, therefore, the BA concentration in aqueous phase was very low, and the probability of new oligomer nucleation was very rare. At this time, latex particle growth become dominate, which caused the increase of particle size for each growth. Since the probability of each latex particle growing up was random, so the latex particle size distribution became wider.

The number of latex particles at the initiation and termination of polymerization are compared in Table VI. The results showed that although the number density of latex particles decreased after latex particles growth, the number of particles at the termination of polymerization was increased slightly, which indicated that some secondary particles were generated. Although oligomer nucleation and particle growth reactions occurred simultaneously during the latex particle growth process, the number of newly generated latex particles is small, again indicating the dominance of the particle growth reaction.

Effect of hardness of shell polymer on the surface morphology of coating

MMA-AN and BMA-AN were used as co-polymerization monomers, the effect of shell hardness of core-shell latex particles on the glass transition temperature (T_g), surface morphology and gloss of

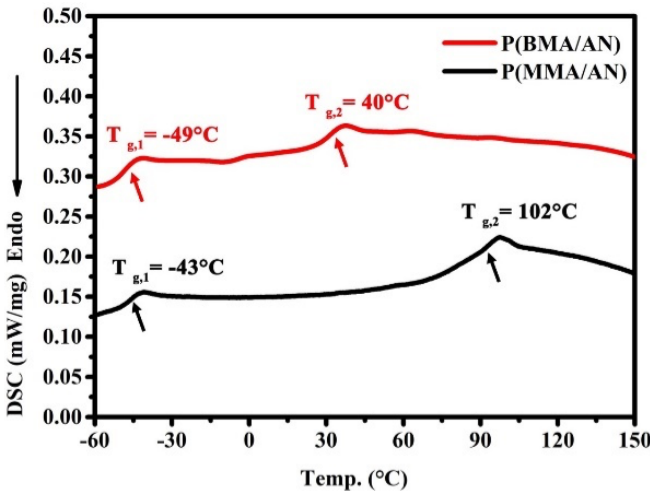

Figure 6. DSC curve of acrylic resin from different shell polymer

Table VI

Glass transition temperature and gloss of films with soft shell and hard shell

Shell structure	Soft shell P(BMA/AN)	Hard shell P(MMA/AN)
Homopolymer T_g (°C)	20(BMA)/96(AN)	105(MMA)/96(AN)
Copolymer theoretical T_g (°C)	50	100
Copolymer practical T_g (°C)	40	102

coating were investigated. DSC curves are shown in Figure 6 and the SEM image are shown in Figure 7, and gloss and glass transition temperature data are shown in Table VII.

DSC was utilized to analyze the glass transition temperature of both acrylic resins with different shell structure. For P(BA-BMA/AN) emulsion, the $T_{g,1}$of core polymer is -49°C, and the $T_{g,2}$ of shell copolymer is 40°C, whilst for P(BA-MMA/AN), the corresponding $T_{g,1}$ and $T_{g,2}$ are -43°C and 102°C. The glass transition temperature of homopolymer PBA, PMMA, PBMA and PAN are -56°C, 105°C, 20°C and 96°C, separately. The glass transition temperature of shell copolymers (T_g) can be calculated by the given FOX[23] formula Equation 6.

$$\frac{1}{T_g} = \frac{W_A}{T_{g,A}} + \frac{W_B}{T_{g,B}} \quad (6)$$

Where T_g is the glass transition temperature of A and B monomer copolymer; W_A and W_B are the mass proportion of A and B monomer in all monomers, respectively; $T_{g,A}$ and $T_{g,B}$ are the glass transition temperatures of A and B monomer homopolymer, respectively.

The $T_{g,1}$ obtained from the practical test deviated from the theoretical value T_g of PBA. The reason for this phenomenon was that the synthesized latex particles were core-shell structure, and the hard-shell structure with higher glass transition temperature outside enveloped the soft core of PBA, so it would make the T_g of PBA core have a certain elevation. The glass transition temperature of copolymers could be calculated by FOX formula. The deviation of the calculated results from the practical results might be due to the actual ratio of the two copolymer monomers deviating from the feed ratio in the continuous polymerization. The observed lower glass transition temperature peak $Tg_{,1}$ corresponded to the PBA core, and the higher $Tg_{,2}$ was similar to the glass transition temperature of the copolymer obtained from theoretical calculations, which showed a better fit with the core-shell model.

The surface morphology of latex film with different shell structure was observed by SEM (Figure 7). It can be seen that latex film with relative soft shell shows smooth surface, whilst latex film with hard shell shows an uneven "pebble-like" surface. Just as mentioned above, the harder shell layer could prevent the latex particles from deformation and fusion in process of drying, which was beneficial for achieving the roughness of coating surface. Compared with MMA, the side chain of BMA was longer and its glass transition temperature was lower. The copolymer composed of BMA and AN had formed a soft-shell layer, which appeared in a rubbery state during film formation, in this case the deformation and fusion of latex particles occurred easily during the film formation process, thus forming a smooth surface of coating. While the copolymer composed of MMA and AN had formed a hard-shell layer, and this hard shell was difficult to move and could fully resist the deformation and fusion of the latex particles during the film formation process, so the latex particles were forced to form the pebble-like shape after film formation.

Effect of cross-linking on the surface morphology and gloss of the coating

Crosslinking of shell copolymer is closely related to latex particle size, glass transition temperature of polymer as well as apparent

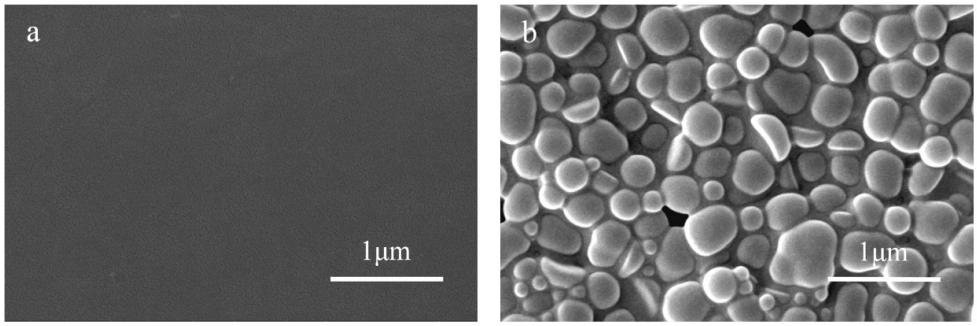

Figure 7. SEM images of acrylate resin films: **(a)** soft shell, **(b)** hard shell

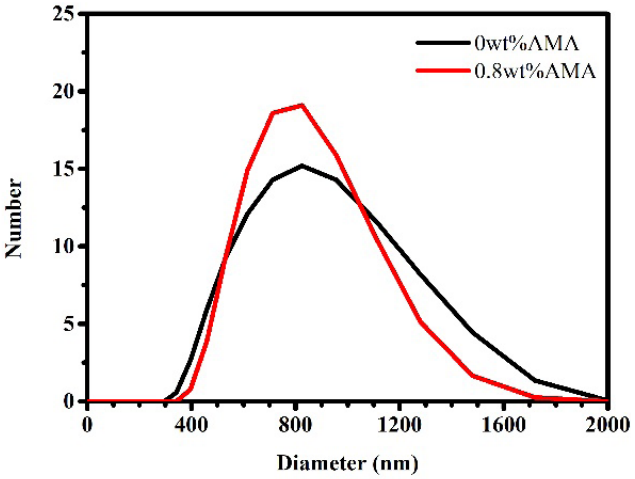

Figure 8. Particle size distribution of P(BA-MMA/AN) core-shell latex particle with or without AMA cross-linking

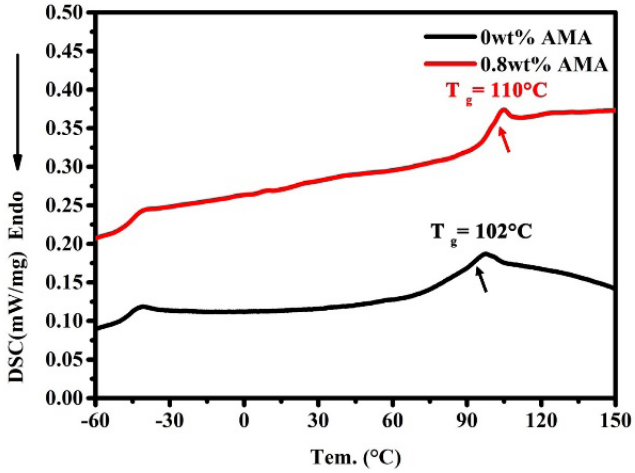

Figure 9. DSC curve of acrylic resin films with or without AMA cross-linking

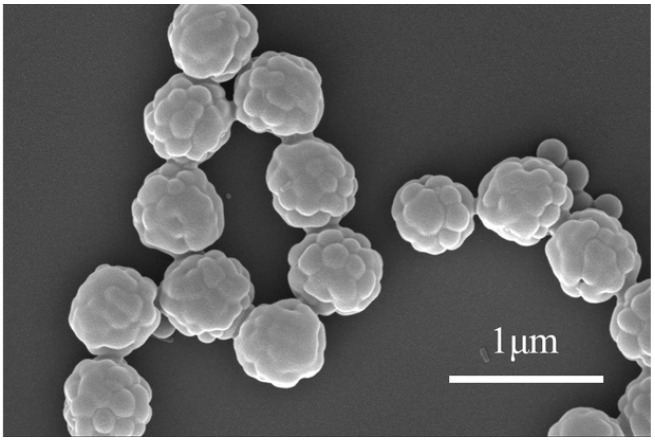

Figure 10. SEM images of acrylic resin films with AMA cross-linked

morphology and gloss of coating. Figure 8 shows the change in particle size of P(BA-MMA/AN) core-shell latex before and after cross-linking, the changes in glass transition temperature of shell copolymer and morphology of P(BA-MMA/AN) coating surface are shown in Figure 9 and Figure 10, Table VIII lists the relative data.

As can be seen from Figure 8 and Table X that the latex particle size shows little changes except the narrowing down of particle size distribution after cross-linking. From Figure 9 it was found that the glass transition temperature of the shell copolymer increased from 102°C to 110°C with the addition of the cross-linking agent, which will further hinder the deformation and fusion of latex particles during the film formation process and thus form a higher roughness of coating surface.

The change of morphology of film surface also proves the above inference. As could be seen from Figure 10, the original pebble-like particles evolved into spherical shape, and separated from each other. The cross-linking also imparts the coating surface sulcus and gyrus structure due to difference in internal stress.

Figure 11 are the AFM images showing the apparent roughness of coating surface. It can be seen that the coating roughness R_q increased rapidly with the increase of particle size of emulsion. For example, the R_q is 144.96nm for emulsion a with particle size 243.98nm but are 173.2 nm, 207.8 nm, 243.98 nm for emulsion b, c, d with increased particle size. This enhanced roughness of coating surface was believed to further improve the diffuse reflection of light, which was conducive to the improvement of the matting property of the coating.

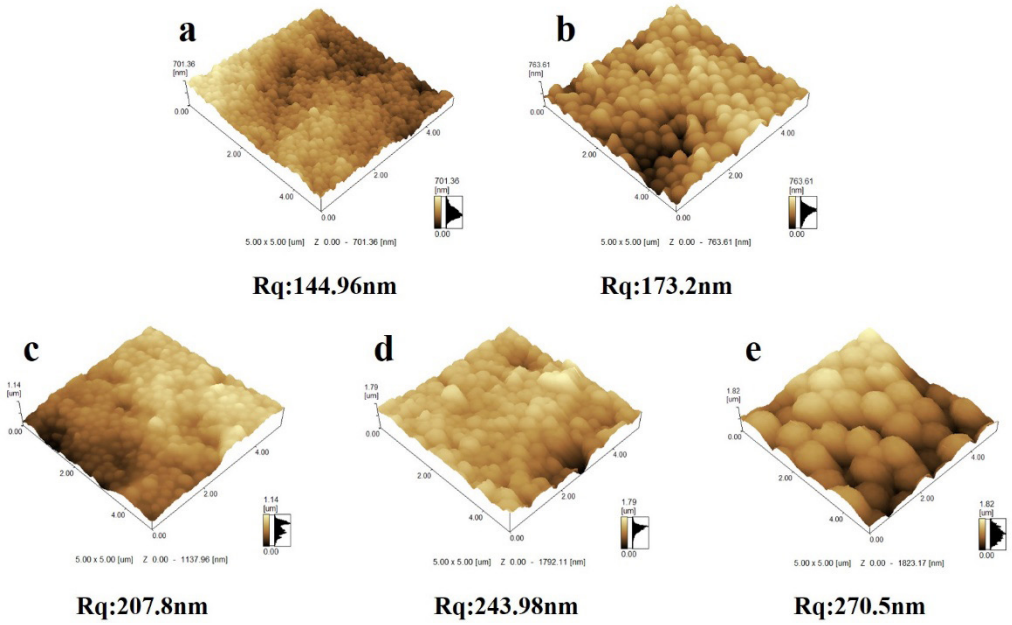

Figure 11. Effect of latex particle diameter and cross-linking on coating roughness: particle size of emulsion **(a)**245.8nm **(b)**359.4nm **(c)**555.8nm **(d)**802.4nm **(e)**804.7nm with AMA cross-linking

Table VIII

Coating roughness, Theoretical light reflectivity and Gloss with different acrylic resin coating

	0wt%AMA				0.8wt%AMA
Acrylic resin coating	**a**	**b**	**c**	**d**	**e**
Particle diameter of emulsion (nm)	245.8	359.4	555.8	802.4	804.7
Coating roughness(nm)	144.96	173.2	207.8	243.98	270.5
Theoretical light reflectivity(R)	22.29	12.65	5.71	2.04	0.90

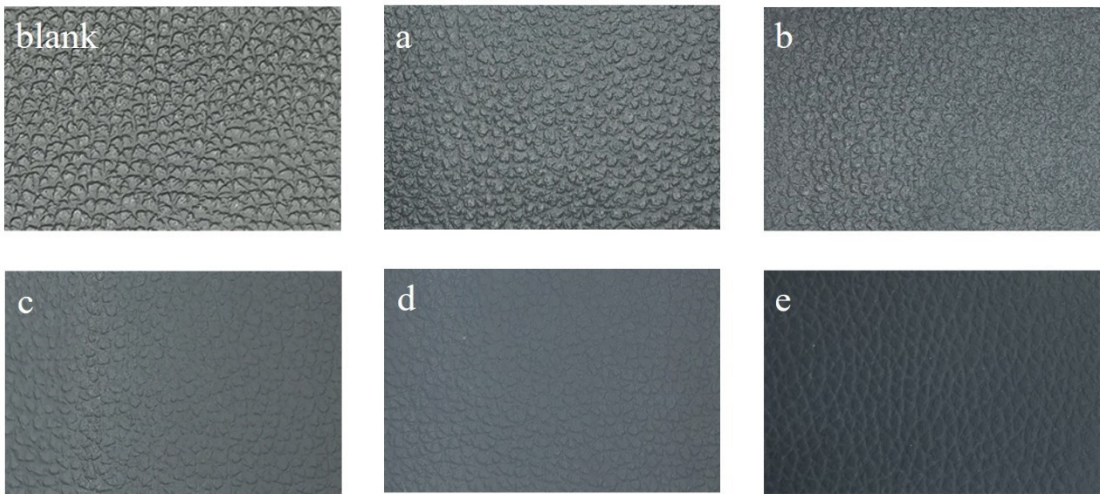

Figure 12. Effect of latex particle diameter and cross-linking on coating gloss: particle size of emulsion **(a)**245.8nm **(b)**359.4nm **(c)**555.8nm **(d)**802.4nm **(e)**804.7nm with AMA cross-linking

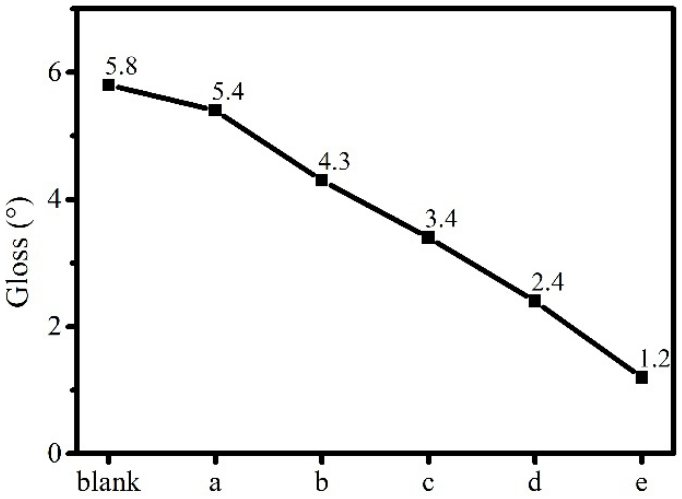

Figure 13. Gloss of finished leather corresponding to Figure 12; particle size of emulsion **(a)**245.8nm **(b)**359.4nm **(c)**555.8nm **(d)**802.4nm **(e)**804.7nm with AMA cross-linking

Based on the R_q measured by AFM, the theoretical light reflectance R of the coating can be calculated by the Equation 1, and its value was shown in Table VIII.

As described in Table VIII, with the increase of surface roughness from 144.96 nm to 270.5 nm, the theoretical light reflectance of the coating calculated by Equation 1 decreased from 22.29 % to 0.9%, showing a significantly decreasing tendency.

Figure 12 and Figure 13 shows the comparison of the gloss of leather coating. It can be seen that the coating exhibits good matting properties. And the gloss of the coating decreased from 5.4° to 2.4° with the increase of the latex particle size form 245.8 nm to 802.4 nm, showing a decreasing tendency. Emulsion d (802nm) and emulsion e (804nm) had similar particle sizes, but the latter exhibited lower gloss (1.2°) and higher matting effect, this is attributed to the crosslinking of shell copolymer. The shell copolymers without crosslinking were looser to each other, after cross-linking, the linear copolymers became network copolymers, which led to the increase of the shell layer densities. As a result, the latex particles were not easily deformed and fused when the coating were drying. Therefore, the coating gloss was further decreased from 2.4° to 1.2°, variation of coating gloss keeps good consistent with the trend of the surface roughness.

Conclusion

In this study, the methods of acrylic latex particle size growth, the effects of different feeding methods on the latex particle size as well as the effects of latex particle size, core-shell structure and crosslinking degree on the apparent morphology and gloss of the coating were investigated. In comparison with batch feeding method, the particle size of PBA seed emulsion prepared from semi-continuous feeding method increased from 82.3nm to 213.4nm. The latex particle size can be further enlarged to 700nm after three-time consecutive growths. More interestingly, the core polymerization still follows the oligomer nucleation mechanism, the newly generated latex particles are less, and the particle growth reaction is the dominant. After shell polymerization, the particle size of resultant emulsion can be increased to 804 nm. Larger latex particle size makes the coating surface present a spherical rough structure after drying, and designable matting effect of the coating can be obtained. The gloss of the coating can also be regulated by changing the hardness and crosslinking of shell copolymer. Compared with P(MBA-AN) with soft-shell structure or without crosslinking, P(MMMA-AN) with hard-shell structure and crosslinking was found to possess lower gloss and higher matting effect. Higher hardness and crosslinking will hinder the deformation and fusion of latex particle during the drying process of the coating, as a result, the surface roughness of the coating will be increased and the leather gloss can be further reduced to below 1.0°.

Acknowledgements

The authors gratefully acknowledge the financial support from National Natural Science Foundation of China (Project No2217080961), the Key Research and Development Program of Shandong Province (Project No: 2019JZZY010355), the Synthetic Leather and High-Performance fibers Innovation Team (2020SCUNG122).

Authors' contributions

Hao Peng: Conceptualization, Methodology, Formal analysis, Writing - Original Draft, Data curation, Formal analysis, Huan Wei: Validation, Investigation, Jun Xiang: Writing- Reviewing, Editing, Validation, Yi Chen: Visualization, Validation, Haojun Fan: Writing - Review & Editing, Supervision.

Funding

This research was supported by National Natural Science Foundation of China (Project No2217080961), the Key Research and Development Program of Shandong Province (Project No: 2019JZZY010355).

Availability of data and materials

All data generated or analyzed during this study are included in this article.

Declarations

Competing interests

The authors declare no competing interest.

References

1. Nungesser E, Hoefler J.; Enhanced acrylic technology for automotive topcoat finishes *JALCA*, **100**(2): 54-60, 2005.
2. Ma Jianzhong, Hu Jing, Zhang Zhijie, et al.; The acrylic resin leather coating agent modified by nano-SiO2J. *Journal of Composite Materials*, **40**(24): 2189-2201, 2006.
3. Zhao Mingyang, Chil-Pin Hsu, Frederic Bauchet, et al.; Low VOC thermosetting polyester acrylic resin for gel coat: US8546486B2P. 2009-05-19.
4. Jiao Cuiyan, Sun Li, Shao Qian, et al.; Advances in Waterborne Acrylic Resins: Synthesis Principle, Modification Strategies, and Their Applications. *ACS Omega*, **6**(4): 2443-2449, 2021.
5. Oll Luis, Frias Aroha, Sorolla Silvia, et al.; Study of the impact on occupational health of the use of polyaziridine in leather finishing compared with a new epoxy acrylic self-crosslinking polymer. *Progress in Organic Coatings*, **154**:106162, 2021.
6. Wang Bingqiao, Wu Yang, Liu Ying, et al.; New Hydrophobic Organic Coating Based Triboelectric Nanogenerator for Efficient and Stable Hydropower Harvesting *ACS Applied Materials & Interfaces*, **12**(28): 31351-31359, 2020.
7. Xie Taoling, Kao Weiyao, Sun Liying, et al.; Preparation and characterization of self-matting waterborne polymer-An overview. *Progress in Organic Coatings*, **142**:105569, 2020.
8. Kumermanis M, Rudzītis J.; Precision Assessment of Surface Coating Roughness Height 3D Parameter St, *Solid State Phenomena*, **199**:155-8, 2013.
9. Yong Qiwen, Chang Jinming, Liu Qi, et al.; Matting Polyurethane Coating: Correlation of Surface Roughness on Measurement Length and Gloss, *Polymers*, **12**(2):326, 2020.
10. Sun Zhe, Fan Haojun, Chen Yi, et al.; Synthesis of self-matting waterborne polyurethane coatings with excellent transmittance, *Polymer International*, **67**(1):78-84, 2018.
11. Yong Qiwen, Liang Caizhen; Synthesis of an Aqueous Self-Matting Acrylic Resin with Low Gloss and High Transparency via Controlling Surface Morphology. *Polymers*, **11**(2):322, 2019.
12. Liu Qi, Liao Bing, Pang Hao, et al.; Preparation and characterization of a self-matting coating based on waterborne polyurethane-polyacrylate hybrid dispersions. *Progress in Organic Coatings*, **143**:105551, 2020.
13. Lin Zhixian, Sun Zhe, Xu Chengping, et al.; A self-matting waterborne polyurethane coating with admirable abrasion-resistance. *RSC Advances*, **11**(14):27620-27626, 2021.
14. Xie Taoling, Kao Weiyao, Zhang Zetian, et al.; Synthesis and characterization of organosilicon modified self-matting acrylate polymer: Insight into surface roughness and microphase separation behavior. *Progress in Organic Coatings*, **157**:106300, 2021.
15. Marcel Visschers, Jozua Laven, van der Linde; Film formation from latex dispersions. *Journal of Coatings Technology*, **73**(916): 49-55, 2001.
16. Keddie Joseph L.; Film formation of latex. *Materials Science and Engineering*, **21**(3): 101-170, 1997.
17. Marcel Visschers, Jozua Laven, Anton L.; Current understanding of the deformation of latex particles during film formation. *Progress in Organic Coatings*, **30**(1-2): 39-49, 1997.
18. Sajjadi S, Jahanzad F.; Comparative study of monomer droplet nucleation in the seeded batch and semi batch mini emulsion polymerization of styrene. *European Polymer Journal*, **39**(4):785-794, 2003.
19. R.G. Gilbert; Emulsion Polymerization: A Mechanistic Approach. London: Academic Press, 1995.
20. Sajjadi S.; Particle formation under monomer-starved conditions in the semi batch emulsion polymerization of styrene. I. Experimental. *Journal of Polymer Science Part A-Polymer Chemistry*, **39**(22):3940-3952, 2001.
21. Sajjadi S.; Particle formation under monomer-starved conditions in the semi batch emulsion polymerization of styrene. Part II. Mathematical modelling. *Polymer*, **44**(1):223-237, 2003.
22. Huang Wenxin, Mao Zepeng, Xu Zhiren; Synthesis and characterization of size-tunable core-shell structural polyacrylate-graft-poly(acrylonitrile-ran-styrene) (ASA) by pre-emulsion semi-continuous polymerization. *European Polymer Journal*, **120**:109247, 2019.
23. Fox T. G., Flory P. J.; 2nd-order transition temperatures and related properties of polystyrene.1. influence of molecular weight. *Journal of Applied Physics*, **21**(6):581-591, 1950.